

Back to Belgium Grants

Final Report

Name of the researcher	Vanessa FIVET
Selection Year	2012
Host institution	Université de Mons
Supervisor	Dr P. Quinet
Period covered by this report	from 01/09/2013 to 31/08/2015
Title of the project	Investigation of atomic processes in lowly-ionized iron-peak and neutron-capture elements. Applications to the modelling of astrophysical and laboratory plasmas.

1. Objectives of the proposal (1 page)

In regard with their high cosmic abundance, accurate and reliable atomic data for the iron-peak elements ($21 < Z < 28$) are of crucial importance in astrophysics. The advent of high-resolution astrophysical spectroscopy lead to the observation of these elements in low ionization stages in various astronomical objects. The interpretation of such high-resolution spectra requires accurate radiative and collisional data for all the iron-group elements. Emission lines of lowly-ionized Fe-peak species have been observed in several nebular environments.

Recent Hubble Space Telescope/Space Telescope Imaging Spectrograph (HST/STIS) observations from the Weigelt blobs of the luminous blue variable star (LBV) Eta Carinae have revealed hundreds of allowed lines and several forbidden lines of singly and doubly-ionized Cr, Mn, Fe, Co and Ni [1]. Lines of lowly-ionized species have also been detected in various galactic sources such as Herbig-Haro objects in the Orion Nebula [2] and extra-galactic objects such as active galactic nuclei [3]. Reliable radiative data are therefore essential for the interpretation of such observations, to obtain a diagnostic of the physical conditions and to model the astrophysical plasma.

The main objective of this project was to use state-of-the-art numerical methods to solve Schrodinger and/or Dirac equations to get an accurate depiction of the electronic structure of iron-peak ions and, therefore, to infer reliable lifetimes and oscillator strengths for those ions.

Another objective of this project was to obtain collisional data for transition elements and in particular iron which is the most abundant transition element in the Universe. The collisional data, together with the energy levels and oscillator strengths also computed in this work, will be useful to the astrophysics community to improve the new generation of non-local thermodynamic equilibrium (NLTE) stellar models [4,5]. Those models can yield much better agreement with the observed stellar spectra but due to their increased complexity, when using inaccurate atomic data, they bear the risk of introducing systematic errors to the analysis [6].

2. Methodology in a nutshell (1 page)

Despite the astrophysical interest of neutral and lowly ionized Fe-peak elements, their atomic properties are still insufficiently accurate or completely unknown. The difficulty in computing accurate atomic data for these ions is common to all neutral and near-neutral transition elements with ground configurations of the type $3d^n 4s^p$. The main reason is the collapse of the $3d$ orbital, which causes competition between filling of the $3d$ and $4s$ subshells. Thus, the single electron approximation that identifies individual electrons with specific orbitals breaks down [7]. To remedy this situation, methods based on the single-electron approximation must also include extensive configuration interaction (CI) and level mixing, which results in extremely large computations owing to the large number of levels arising from the open $3d$ subshell.

In the present project, we proposed the simultaneous use of different theoretical methods based on different approximations to study those complex electronic structures. This multiplatform approach was unique to this project and has proven successful in many previous studies performed within the same collaboration such as those concerning the K shells of Fe, O, Ne, Mg, Si, S, Ar, Ca, and Ni ions (see e.g. [8,9]) and the electron impact excitation of Fe III [10]. This has the advantage that it allows for consistency checks and intercomparison. It also helps to reveal which physical processes are important for any given transition, since different platforms employ different treatments of, for example, relativistic effects and orthogonal vs. non-orthogonal orbitals.

For the atomic structure calculations, the methods employed were the pseudo-relativistic Hartree-Fock (HFR) approach [11], the fully relativistic multi-configuration Dirac-Fock (MCDF) method [12-14] and the Thomas-Fermi-Dirac potential approximation implemented in the AUTOSTRUCTURE (AUTOS) [15] codes. Note that HFR and AUTOS methods were combined with a semi-empirical adjustment of the calculated energies to the experimental values.

For allowed transitions, we computed the oscillator strengths using only the HFR method and, instead of benchmarking the results against other theoretical methods, we performed experimental lifetime measurements using the laser-induced fluorescence technique in collaboration with the Lund Laser Centre in Lund, Sweden.

The scattering calculations have been carried out with the R-matrix technique within the close-coupling approximation. This R-matrix method has been implemented into the RMATRIX package [16] and the DARC package [17]. RMATRIX computes cross sections in LS-coupling, but allows for relativistic corrections through the Breit-Pauli approximation. The newest version of the parallelized package allows for computations that are orders of magnitude larger than possible just a few years ago [18]. DARC is a fully relativistic Dirac-Coulomb R-matrix code, which is essential for the calculations in heavier elements where the relativistic effects are expected to play a major role.

3. Results (8-10 pages)

3.1 Radiative and collisional data for Fe II

3.1.1 Radiative data

Reliable quantitative spectral modelling of singly ionized iron (Fe II) is of paramount astrophysical importance since various fundamental research areas (e.g. active galactic nuclei, cosmological supernova light curves, solar and late-type-star atmospheres, and gamma-ray-burst afterglows) depend on such models. This ion has gained even more attention in recent years with the advent of large-scale observational surveys as well as deeper and high-resolution spectroscopy.

Fe II spectral modelling firstly requires the detailed treatment of electron impact excitation of metastable levels followed by spontaneous decay through dipole forbidden transitions. The computation of accurate electron impact collision strengths and A-values has proven to be cumbersome despite many efforts over several decades. This difficulty in describing the Fe II ion is mostly due to the complexity of the effective potential acting on the $4s$, $3d$ and $4p$ electrons.

Realistic representations of the atomic structure are needed to obtain accurate energy levels, line wavelengths, and A-values, but also because such representations are the basis of reliable scattering calculations. For this work, we used a combination of numerical methods: the pseudo-relativistic Hartree–Fock (HFR) code of Cowan, the Multi-configuration Dirac–Fock (MCDF) code and the scaled Thomas–Fermi–Dirac central-field potential as implemented in AUTOSTRUCTURE. The present effort was focused on the computation of transition probabilities (A-values) for forbidden lines between the 52 lowest even levels belonging to the $3d^7$, $3d^64s$ and $3d^54s^2$ configurations.

The HFR configuration expansion included 12 configurations and was based on the 10-configuration calculation by Quinet *et al.* [19] with the addition of $3d^54d^2$ and $3s3p^63d^64s^2$. The radial parts of the multi-electron Hamiltonian were adjusted empirically using a least-square fit procedure to better reproduce energy levels for the configurations $3d^7$, $3d^64s$ and $3d^54s^2$. This yields a very good agreement between theoretical and experimental energy level (78 cm^{-1} in average).

Regarding the AUTOS calculations, we used not only the original code but also the version modified by Bautista [20] with non-spherical multipole corrections to the Thomas-Fermi-Dirac-Amaldi potential (later called TFDAC). For the present work, we found necessary to limit the potential to a single dipole correction and, more importantly, the radial dependence of this dipole correction was scaled by an additional parameter (giving rise to the new-TFDAC method). We performed four different AUTOS calculations. Two of them were built on the configuration expansion used by Bautista and Pradhan [21] and made use of both the TFDAC and new-TFDAC method. One considered an expansion similar to the HFR one previously described. The last one was considerably smaller with only 7 configurations and was comparable with the expansion used for the smaller MCDF calculation with the addition of a $4d$ pseudo-orbital. It was observed that the new correction to the potential improved significantly the quality of the theoretical energy levels with regards to the experimental values. The two smaller models, as expected, yield poorer results in term or energy level accuracy.

For the MCDF calculation, we tested two different models with 6 and 12 configurations respectively. However, giving the difficulty of obtaining convergence for the $4d$ orbital, none of our models included this important orbital. This resulted in a rather poor quality of energy levels when using the MCDF method. We nevertheless decided to use the smaller target to perform scattering calculations with the fully relativistic R-matrix code DARC (calculations with the 12-configuration target are still out of our reach with the computational power available nowadays). It is noted that we wrote a programme to use a converged $4d$ AUTOS orbital within the MCDF code but this procedure didn't improve the agreement between theoretical and experimental energies.

By studying the dispersion of the transition probabilities obtained through the various independent numerical methods, we established a set of recommended values together with an estimation of the uncertainties affecting those values. We were able to show that the lifetimes for the lowest 16 levels of Fe II, which are responsible for the infrared and mid-infrared spectra, are known within 10% or better. The lifetimes for higher levels, which yield the optical spectrum, have uncertainties that range between 10 and 30%. Figure 1 shows the estimated uncertainties on both the branching fractions and the A-values. It is noted that about two third of the branching ratios seem to be constrained within 20%. However, very few transitions (about 2% of the total set) have an A-value with an uncertainty of 10% or better. On the positive side, almost three quarter of the A-values computed are constrained within 30%. We thus expect that the majority of observable lines and transitions regulating the ion population balance are sufficiently accurate.

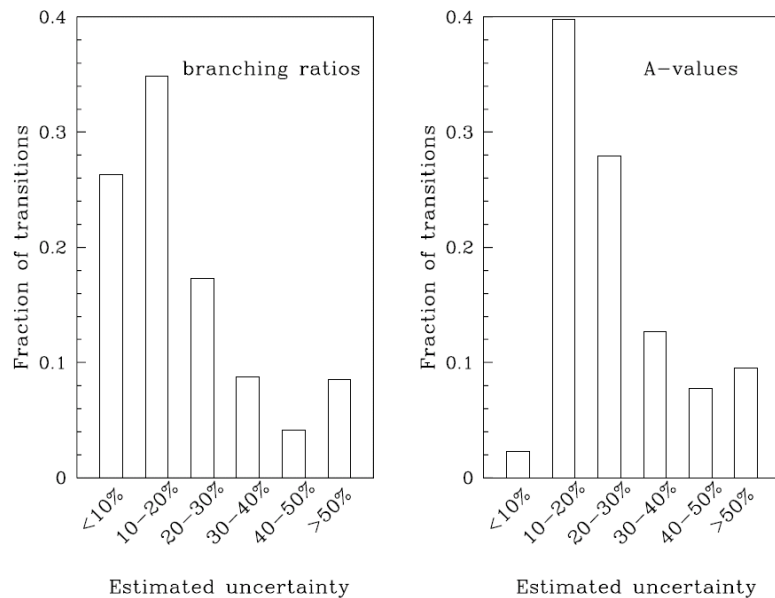


Figure 1: Branching ratio and A-values error distributions for dipole forbidden transitions among metastable levels of Fe II.

3.1.2 Comparison with astrophysical spectra

In order to benchmark our theoretical results against astrophysical spectra, we compared observed and theoretical intensity ratios between emission lines arising from the same upper level. The advantage of looking at these ratios is that they depend only on A-values regardless of the physical conditions of the plasma. Therefore, the ratios ought to be the same in any source spectra, provided the spectra have been corrected for extinction.

Fe II yields the richest spectrum of any astronomically abundant chemical species; thus, its high-resolution optical and near-IR forbidden lines are the best suited for the present evaluation. In the present work, we used HST/STIS archived spectra of the Weigelt blobs of η Carinae, deep echelle spectrum ($R = 30\,000$) of the Herbig–Haro object (HH 202) in the Orion Nebula [2] and the X-shooter spectrum of the jet of the pre-main-sequence star SEO-H 574 [22].

In order to evaluate quantitatively the comparison of theoretical (R_{th}) and observed line (R_{ob}) ratios when taking into account the respective uncertainties, we computed the statistical χ^2 indexes defined as:

$$\bar{\chi}^2 = \sqrt{\frac{1}{N} \sum \frac{(R_{ob} - R_{th})^2}{(\delta R_{ob}^2 + \delta R_{th}^2)}}$$

According to that definition, an index of 1 indicate a perfect estimation of the uncertainties. If it is greater than one, the uncertainties are underestimated (and similarly, overestimated if $\chi^2 < 1$).

We can see in Table 1 a comparison of the different χ^2 indexes calculated for the various computations performed in this work. We see that the introduction of the new correction in the TFDA potential drastically improved the agreement with the observations. It is also noted that, although relatively simple, the AUTOS model with 7 configurations yields the best agreement with the astrophysical line ratios. But the most interesting result is undoubtedly that when taking into account estimated uncertainties for the theoretical values, we improve considerably the agreement.

Calculation	χ^2
HFR	5.16
AUTOS TFDAc	358
AUTOS new-TFDAc	4.92
AUTOS HFR-like model	12.64
AUTOS 7configs	4.10
Recommended values (without uncer.)	4.34
Recommended values (with uncer.)	1.38

Table 1: Comparison of theoretical and observed branching ratios for the different calculations carried out in this work.

It is unclear if the remaining line ratio discrepancies (in red) arise from observation or theory; nonetheless, as show in Figure 2, the overall agreement between theory and observations is satisfactory.

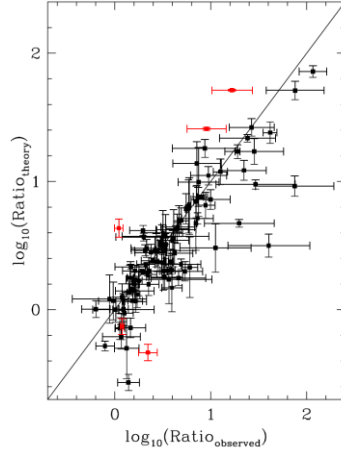


Figure 2: Comparison of theoretical and observed intensity ratios for lines arising from the same upper level.

3.1.3 Electron impact collision strengths

We carried out electron impact excitation calculations with the different Fe II target expansions described above using the R-matrix code with intermediate frame transformation (RM+ICFT) and the fully-relativistic R-matrix code (DARC). Figure 3 shows a collision strength cross section obtained for the transition from the ground level ${}^6D_{9/2}$ to the first excited level ${}^6D_{7/2}$.

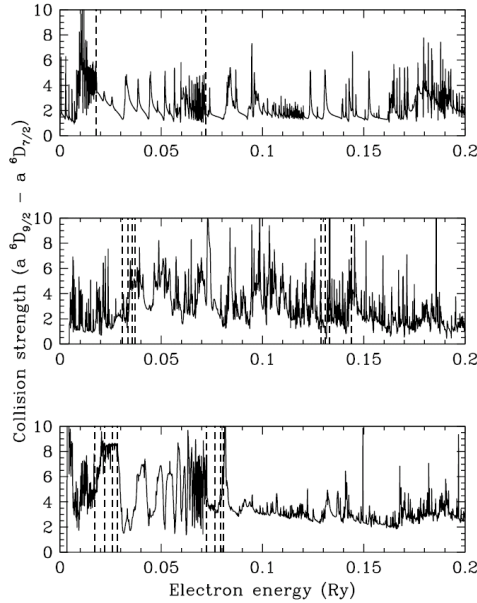


Figure 3: collision strength from the $3d^6 4s {}^6D_{7/2}$ to the ground level ${}^6D_{9/2}$. The top panel show the RM+ICFT calculation performed with the 'new-TFDac' target. The middle and bottom panels are the DARC calculations, respectively without and with the thresholds shifted to laboratory energies

In order to assess the collisional data quality, we constructed collisional excitation models with the recommended A-values (see section 3.1.1) and the effective collision strength computed here. The line emissivities were then compared to observation in the Herbig-Haro object HH 202 [2]. Atomic rate error propagation in predicted line emissivities has been calculated with a technique we elaborated several years ago [23]. We observed a nearly perfect statistical agreement between theory and observations when all uncertainties are well accounted for.

3.2 Forbidden transition probabilities for doubly-ionized iron-peak elements

In the present project, we carried out the first systematic study of the electronic structure of doubly-ionized Fe-peak species. The magnetic dipole (M1) and electric quadrupole (E2) transition probabilities were computed using the pseudo-relativistic Hartree-Fock (HFR) code of Cowan and the central Thomas-Fermi-Dirac-Amaldi potential approximation implemented in AUTOSTRUCTURE. As described in section 2, this multi-platform approach allows for consistency checks and intercomparison and has proven very useful for estimating the uncertainties affecting the radiative data.

We obtained more than 550 transition probabilities contributing to the depopulation of the metastable levels belonging to the $3d^k$ and $3d^{k-1}4s$ configurations (with $k=1-8$ for $Z=21-28$).

For both physical models, we chose to introduce the same set of configurations: $3d^k$, $3d^{k-1}4s$, $3d^{k-1}5s$, $3d^{k-1}4d$, $3d^{k-2}4s^2$, $3d^{k-2}4p^2$, $3d^{k-2}4d^2$, $3d^{k-2}4s4d$, $3d^{k-2}4s5s$, $3s3p^63d^{k+1}$, $3s3p^63d^k4s$ and $3s3p^63d^{k-1}4s^2$ (with $k=1-8$ for $Z=21-28$). Since the AUTOS method uses orthogonal orbital, each configuration is described by the same set of orbitals. Therefore, in order to get a better representation of the $4p$ orbital, we added two configurations to our Thomas-Fermi model: $3d^{k-1}4p$ and $3d^{k-2}4s4d$.

For the HFR calculations, we applied the least-square optimization routine to minimize the energy differences between the theoretical and the available experimental energy levels belonging to the low-lying even configurations $3d^k$ and $3d^{k-1}4s$.

When performing AUTOS calculations, it is customary to adjust every scaling parameter λ_{nl} independently from each other. For this work, we chose to apply a new technique consisting of optimizing together the scaling parameters of the core orbital ($1s$, $2s$, $2p$, $3s$ and $3p$) to simulate the effect of missing open-core configurations in our model.

The overall agreement between our two independent theoretical methods was about 10-15% and we observed a similar agreement with the few previous theoretical results available in the literature.

Table 2 shows an example of the transition probabilities computed for transition arising between the three metastable levels of Sc III ($Z=21$). The results of our calculations are compared to one of the calculation previously available in the literature [24]. Those comparisons allowed for further consistency checks. The agreement was found to be excellent (within 10%).

Lower level	Upper level	λ (nm)	Type	A(M1+E2) (s^{-1})		
				HFR	AUTOS	Other [25]
$3d^2D_{3/2}$	$3d^2D_{5/2}$	50597.04	M1+E2	8.36[-5]	8.33[-5]	8.33[-5]
$3d^2D_{3/2}$	$4s^2S_{1/2}$	391.55	M1+E2	7.67	8.71	7.83
$3d^2D_{5/2}$	$4s^2S_{1/2}$	394.61	E2	11.07	12.56	11.40

Table 2: Transition probabilities for the three metastable levels of Sc III.

Figure 4 shows a comparison of transition probabilities obtained for doubly-ionized titanium ($Z=22$). We can see an excellent agreement (within 10%) between our present HFR and AUTOS results together with the fully-relativistic Multi-Configurational Dirac-Fock (MCDF) calculations of Raassen and Uylings [25]. We also see a systematic discrepancy (around 20%) with the earlier results of Biémont et al. [26] that can be explained by the simpler physical model used by these authors.

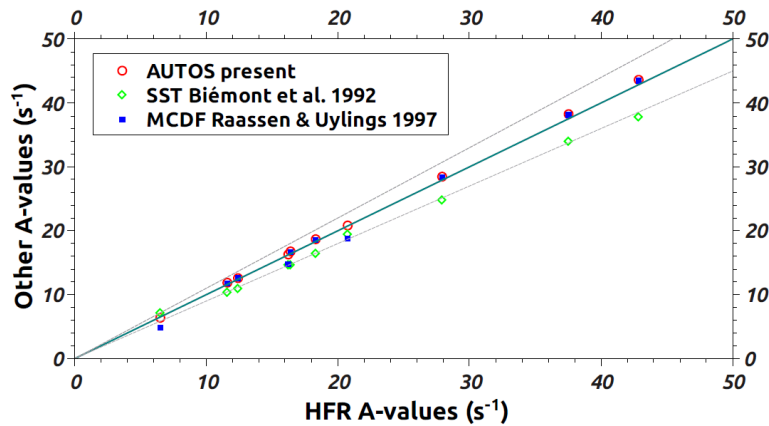


Figure 4: Comparison between our HFR and AUTOS calculations and previous results in Ti III.

An identical plot (see Figure 5) for Fe III ($Z=26$) reveals a slight systematic discrepancy (15 to 20%) between our HFR calculation and the data obtained with the AUTOS code. However, we can see that the agreement between our AUTOS results and the earlier AUTOS data from Bautista *et al.* [10] is excellent (often within a few percentage points), despite the fact that the earlier model was much more extensive and included 40 configurations. This result gives us confidence that, even though we are using a quite small configuration expansion, it includes the most important physical effects and adding more configurations to the model is unlikely to improve the A-values.

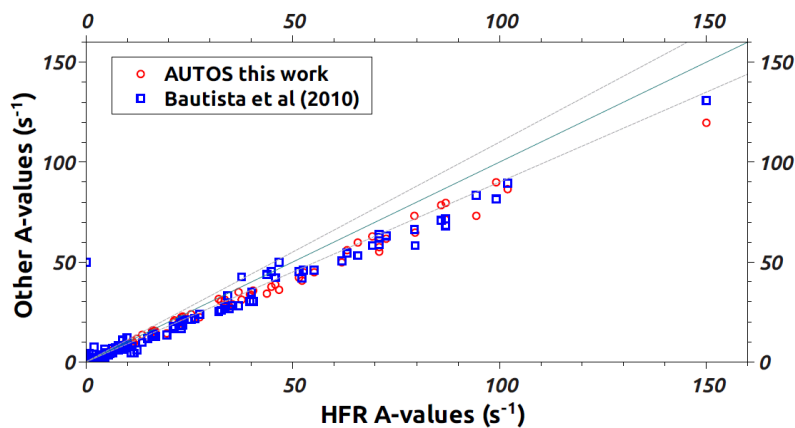


Figure 5: Comparison between our HFR and AUTOS calculations and previous results in Fe III.

3.3 Experimental and theoretical lifetimes for singly-ionized iron-peak ions

In collaboration with our colleagues from the Lund University (Sweden) and the Bulgarian Academy of Science in Sofia (Bulgaria), we started an investigation of the lifetimes of high-lying energy levels of the same parity as the fundamental level.

Abundances determination of lowly-ionized Fe-peak elements in stars serves as an important test of the stellar evolution and supernova explosion models. The high-excitation lines are benchmarking the LTE-modelling of the stellar atmospheres. Along with the development of 3D-atmospheres this is the current challenges for accurate stellar abundances, and the atomic data are important for this development [27, 28].

The lifetime measurements have been performed on the Time-Resolved Laser-Induced Fluorescence (TR-LIF) setup of the Lund Laser Centre. Figure 6 shows a schematic view of this setup, a thorough description can be found in earlier papers (see e.g. [29]). The experimental study of these highly excited levels has been made possible by the use of a novel two-step excitation scheme: the intermediate odd states are excited as a first step and they are used as a platform for excitation of high-lying even parity states under measurements.

The theoretical investigation of these high-lying states is also a challenge: those excited levels are often subject to more configuration mixing than the ground states and it makes their accurate theoretical representation more difficult. An experimental benchmark such as the one provided in this work is therefore welcomed to assess the quality of our calculations.

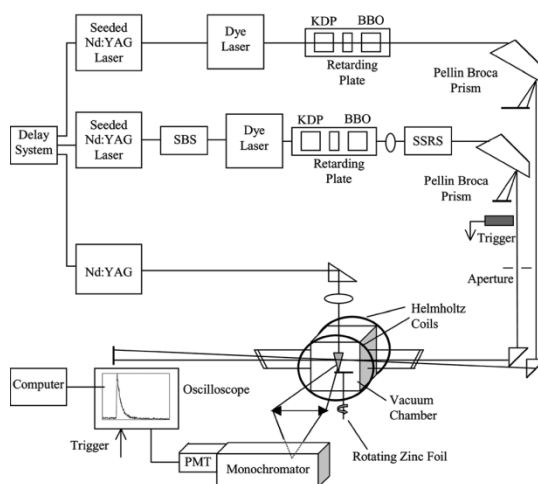


Figure 6: Experimental setup used to measure lifetimes with the TR-LIF at the Lund Laser Centre.

3.3.1 Singly-ionized nickel (Ni II)

The first ionization stage of nickel was the first ion to be considered in this study. As mentioned before, all iron-peak elements play a special role in astrophysics since they represent the final stage of element production in stars. But amongst those elements, nickel is one of the most important one because it has the maximum binding energy per nucleon closely followed by iron.

Calculations of energy levels and radiative transition rates in Ni II have been carried out using the relativistic Hartree-Fock (HFR) approach modified to take core-polarization effects into account (see e.g. Ref [31]). This method (HFR+CPOL) has been combined with a least-squares optimization process of the radial parameters in order to reduce the discrepancies between the Hamiltonian eigenvalues and the available experimental energy levels.

The following 23 configurations were explicitly introduced in the calculations: $3d^9$, $3d^84d$, $3d^85d$, $3d^74s4d$, $3d^74s5d$, $3d^64s^24d$, $3d^84s$, $3d^85s$, $3d^74s^2$, $3d^74s5s$, $3d^64s^25s$ for the even parity and $3d^84p$, $3d^85p$, $3d^74s4p$, $3d^74s5p$, $3d^64s^24p$, $3d^64s^25p$, $3d^84f$, $3d^85f$, $3d^74s4f$, $3d^74s5f$, $3d^64s^24f$, $3d^64s^25f$ for the odd parity.

The ionic core considered for the core-polarization model potential and the correction to the transition dipole operator was a $3d^6$ Ni V core.

The radiative lifetimes measured and computed in the present work are presented in Table 3. The error bars shown include statistical and random errors. About 10 to 20 measurements are performed for obtaining radiative lifetimes of a given states. The average agreement between the theoretical lifetimes and the new experimental lifetimes is about 12%.

Level	Energy (cm ⁻¹) [1]	Radiative lifetime (ns)	
		Experiment (This work)	HFR+CPOL (This work)
$3p^63d^84d^4D_{7/2}$	98467.25	1.27±0.10	1.30
$3p^63d^84d^4H_{13/2}$	98822.55	1.25±0.07	1.32
$3p^63d^84d^4G_{11/2}$	99132.78	1.19±0.15	1.34
$3p^63d^84d^4F_{9/2}$	99154.81	1.12±0.10	1.29
$3p^63d^84d^4G_{7/2}$	100475.82	1.60±0.20	1.33
$3p^63d^84d^4F_{7/2}$	100592.98	1.60±0.15	1.34

Table 3: Experimental and theoretical lifetimes for high-lying levels of the $3d^84d$ configuration of Ni II.

3.3.1 Singly-ionized titanium (Ti II)

Similar calculations and measurements have been carried out in singly-ionized titanium. The following 17 configurations have been considered explicitly in the physical model: $3d^3$, $3d^24d$, $3d^25d$, $3d4s4d$, $3d4s5d$, $3d^24s$, $3d^25s$, $3d4s^2$, $3d4s5s$ (even) and $3d^24p$, $3d^25p$, $3d4s4p$, $3d4s5p$, $3d^24f$, $3d^25f$, $3d4s4f$, $3d4s5f$ (odd).

In order to consider the CPOL corrections in the calculations, a dipole polarizability and a cut-off radius corresponding to a Ti IV ionic core were adopted.

Table 4 presents the 6 lifetimes measured for the $3d^25s e^4F$ states, together as the intermediate level used for the first step of the excitation process. The table also presents the computed values with and with the polarization contributions in order to illustrate the effect of these corrections on the final lifetimes.

Final level	Intermediate level	Exp lifetime (ns)	HFR lifetime (ns)	HFR+CPOL lifetime (ns)
$e^2F_{5/2}$	$z^2D_{3/2}$	3.23 ± 0.2	3.55	3.48
$e^2F_{7/2}$	$z^4D_{7/2}$	3.16 ± 0.2	3.55	3.48
$e^4F_{3/2}$	$z^4F_{5/2}$	2.95 ± 0.2	3.27	3.21
$e^4F_{5/2}$	$z^4F_{5/2}$	3.50 ± 0.2	3.27	3.22
$e^4F_{7/2}$	$z^4F_{9/2}$	3.25 ± 0.25	3.27	3.22
$e^4F_{9/2}$	$z^4F_{9/2}$	3.68 ± 0.25	3.27	3.22

Table 4: Experimental and theoretical lifetimes for high-lying levels of the $3d^25s$ configuration of Ti II.

3.3.1 Singly-ionized cobalt (Co II)

We performed very recently some lifetime measurements following the same method for singly-ionized cobalt. We were able to measure 18 lifetimes for $3d^7(^4F)4p$ and $4d$ configurations (see Table 5). Calculations within the HFR+CPOL framework are currently well underway.

Level	Energy (cm ⁻¹)	Exp lifetime (ns)
$4p z ^5F_3$	45972	3.21 ± 0.15
$4p z ^5F_2$	46452	3.12 ± 0.15
$4p z ^5D_4$	46320	3.10 ± 0.15
$4p z ^5D_3$	47039	3.11 ± 0.15
$4p z ^5D_2$	47537	3.04 ± 0.20
$4p z ^5G_6$	47078	2.70 ± 0.15
$4p z ^5G_5$	47345	2.93 ± 0.15
$4p z ^5G_4$	47807	2.84 ± 0.15
$4p z ^5G_3$	48150	2.86 ± 0.15
$4p z ^5G_2$	48388	2.84 ± 0.15
$4p z ^3G_4$	49348	3.03 ± 0.15
$4d e ^5H_6$	90975	1.57 ± 0.10
$4d e ^5H_5$	91646	1.52 ± 0.10
$4d e ^5G_5$	90697	1.41 ± 0.10
$4d e ^5G_4$	91049	1.35 ± 0.10
$4d e ^3G_5$	91327	1.44 ± 0.10
$4d e ^3H_6$	91623	1.36 ± 0.10
$4d f ^3F_4$	93739	1.58 ± 0.10

Table 5: Experimental Lifetimes for the $3d^7(^4F)4p$ and $4d$ configuration of Co II.

4. Valorisation/Diffusion (including Publications, Conferences, Seminars, Missions abroad...)

During this fellowship, I was given the opportunity to present my work at the 46th Conference of the European Group for Atomic Systems (EGAS-46) in Lille (France). I also attended the 24th International Conference on Atomic Physics (ICAP-24) in Washington D.C. (USA), a conference gathering the world experts in atomic physics amongst which several Nobel Prizes.

I also participated to the experimental campaign for the measurement of radiative lifetimes using the LIF technique which took place at the Lund Laser Centre at the Lund University (Sweden) in June 2015.

a) Posters and communications

- *Radiative data of lowly-ionized iron-peak elements for transitions of astrophysical interest*,
V. Fivet, P. Quinet and M.A. Bautista
46th Conference of the European Group for Atomic Systems (EGAS-46)
Lille, France, 2014
- *Radiative data of lowly-ionized iron-peak elements for transitions of astrophysical interest*,
V. Fivet, P. Quinet and M.A. Bautista
24th International Conference on Atomic Physics (ICAP-24)
Washington D.C., USA, 2014

b) Publications

- *Atomic data and spectral model for Fe II*,
M. A. Bautista, V. Fivet, C. Ballance, P. Quinet, G. Ferland, C. Mendoza and T.R. Kallman
Astrophysical Journal, 808 (2015) 174
- *A detailed and systematic study of radiative rates for forbidden transitions of astrophysical interest in doubly-ionized iron-peak elements*,
V. Fivet, P. Quinet and M.A. Bautista
Astronomy & Astrophysics, submitted for publication (2015)
- *Radiative Parameters for Ni II lines of Astrophysical Interest*,
H. Hartman, L. Engström, H. Lundberg, H. Nilsson, P. Palmeri, P. Quinet, V. Fivet, G. Malcheva and K. Blagoev,
In preparation (2015)
- *Radiative Lifetimes in singly-ionized titanium (Ti II)*,
H. Hartman, L. Engström, H. Lundberg, H. Nilsson, P. Palmeri, P. Quinet, V. Fivet, G. Malcheva and K. Blagoev,
In preparation (2015)

5. Future prospects for a permanent position in Belgium

Due to the lack of permanent position opened in the field of atomic physics in Belgium, I decided to leave academic research and I am currently investigating the Belgian job market.

6. Miscellaneous

During this fellowship, I took part to several outreach programs organized by the Mons University - SciTech² (Printemps des Sciences, exhibit “histoire d'ondes”, workshop “Lumière sur les trous noirs” ...).

I was also involved in teaching activities (practical work for Atomic and Molecular Physics and Atomic Astrophysics) and I co-directed with Dr Quinet a master student for an internship.

References

- [1] Zethson T. *et al.*, *A&A* **540** (2012) 119
- [2] Mesa-Delgado A. *et al.*, *MNRAS* **395** (2009) 855
- [3] Vestergaard M. & Wilkes B.J., *ApJS* **134** (2001) 1
- [4] Asplund M., *ARA&A* **43** (2005) 481
- [5] Przybilla N. *et al.*, *A&A* **445** (2006) 1099
- [6] Przybilla N. and Butler K., *A&A* **379** (2001) 955;
- [7] Connerade J.P., *Highly Excited Atoms*, Cambridge University Press (1998)
- [8] Bautista M.A. *et al.*, *A&A* **403** (2003) 339
- [9] Palmeri P. *et al.*, *A&A* **410** (2003) 359
- [10] Bautista M.A. *et al.*, *ApJ* **718** (2010) L189
- [11] Cowan R.D., *The Theory of Atomic Structure and Spectra*, University of Cal. Press, Berkeley (1981)
- [12] Grant I.P. *et al.*, *Comput. Phys. Commun.* **21** (1980) 207
- [13] Dylla K.G. *et al.*, *Comput. Phys. Commun.* **55** (1989) 425
- [14] Parpia F.A. *et al.*, *Comput. Phys. Commun.* **94** (1996) 249
- [15] Badnell N.R., *J. Phys. B: At. Mol. Opt. Phys.* **30** (1997) 1
- [16] Berrington K.A. *et al.*, *Comput. Phys. Commun.* **92** (1995) 290
- [17] Ait-Tahar S. *et al.*, *Phys. Rev. A* **54** (1996) 3984
- [18] Mitnik D.M. *et al.*, *J. Phys. B: At. Mol. Opt. Phys.* **36** (2003) 717
- [19] Quinet P. *et al.*, *A&AS* **120** (1996) 361
- [20] Bautista M.A., *J. Phys. B: At. Mol. Opt. Phys.* **41** (2008) 065701
- [21] Bautista M.A. & Pradhan A.K. *A&A* **115** (1996) 551
- [22] Giannini T. *et al.*, *ApJ* **778** (2013) 71
- [23] Bautista M.A. *et al.*, *ApJ*, **770** (2013) 15
- [24] Nandy D.K. *et al.*, *J. Phys. B: At. Mol. Opt. Phys.* **44** (2011) 225701
- [25] Raassen A.J.J. & Uylings P.H.M., *A&As* **116** (1997) 573
- [26] Biémont E. *et al.*, *J. Phys. B: At. Mol. Opt. Phys.* **25** (1992) 5029
- [27] Wongwathanarat A. *et al.*, *Proceedings of the IAU*, Vol. **7**, Symposium S279 (2011) 150
- [28] Lind M. *et al.*, *MNRAS* **427** (2013) 50
- [29] Fivet V. *et al.*, *J. Phys. B: At. Mol. Opt. Phys.* **39** (2006) 3587
- [30] Quinet P. *et al.*, *MNRAS* **307** (1999) 934